

# Generative AI for O-RAN Slicing: A Semi-Supervised Approach with VAE and Contrastive Learning

Salar Nouri   Mojdeh Karbalaee Motaleb   Vahid Shah-Mansouri   Seyed Pooya Shariatpanahi

School of Electrical and Computer Engineering, College of Engineering, University of Tehran, Tehran, Iran

{salar.nouri, mojdeh.karbalaee, vmansouri, p.shariatpanahi}@ut.ac.ir

**Abstract**—This paper introduces a novel generative AI (GAI)-driven, unified semi-supervised learning architecture for optimizing resource allocation and network slicing in O-RAN. Termed Generative Semi-Supervised VAE-Contrastive Learning, our approach maximizes the weighted user equipment (UE) throughput and allocates physical resource blocks (PRBs) to enhance the quality of service for eMBB and URLLC services. The GAI framework utilizes a dedicated xApp for intelligent power control and PRB allocation. This integrated GAI model synergistically combines the generative power of a VAE with contrastive learning to achieve robustness in an end-to-end trainable system. It is a semi-supervised training approach that concurrently optimizes supervised regression of resource allocation decisions (i.e., power, UE association, PRB) and unsupervised contrastive objectives. This intrinsic fusion improves the precision of resource management and model generalization in dynamic mobile networks. We evaluated our GAI methodology against exhaustive search and deep Q-Network algorithms using key performance metrics. Results show our integrated GAI approach offers superior efficiency and effectiveness in various scenarios, presenting a compelling GAI-based solution for critical network slicing and resource management challenges in next-generation O-RAN systems.

**Index Terms**—Generative AI, Variational Autoencoder, Contrastive Learning, O-RAN Slicing, Resource Allocation

## 1 INTRODUCTION

Wireless communication has evolved from a convenience to a necessity, driven by the increasing demand for faster and more reliable connectivity across diverse Quality of Service (QoS) requirements [1]. The advent of Fifth Generation (5G) marks a significant leap, enabling applications such as augmented reality and autonomous vehicles [2], while laying the foundation for Sixth Generation (6G), which aims to further redefine global connectivity.

To meet the growing complexity of future networks, 3GPP begins integrating Artificial Intelligence (AI) into core Radio Access Network (RAN) functions such as beam management, positioning, and Channel State Information (CSI) feedback, initiating a shift towards intelligent and adaptive systems. As technologies like extreme Multiple-Input Multiple-Output (MIMO), deep receivers, and deep schedulers emerge, AI becomes essential to handle real-time data-driven tasks such as Physical Resource Blocks (PRBs) allocation and power control in both uplink and downlink [3]–[5].

Network slicing and O-RAN are critical enablers in both 5G and 6G, offering the flexibility to support services like Enhanced Mobile Broadband (eMBB), Ultra-Reliable Low Latency Communications (URLLC), and Massive Machine-Type Communications (mMTC), each with distinct performance demands [4], [6]. In 6G, network slicing will extend to advanced use cases such as holographic communication and tactile Internet, ensuring scalable and adaptable resource management [7], [8]. At the same time, O-RAN—with its open interfaces, disaggregation of hardware and software—provides a modular, cost-effective platform for em-

bedding AI-based control and enabling multi-vendor interoperability [9].

These architectures are foundational for realizing sophisticated AI-driven resource allocation strategies. As network demands grow and QoS requirements diversify, highly adaptive intelligent solutions for dynamic scheduling, power control, and PRB management become increasingly paramount. Effectively integrating such advanced AI within flexible frameworks such as network slicing and O-RAN is crucial to ensure future wireless systems are not only efficient and responsive but also proactively service-aware, making sophisticated AI capabilities indispensable for unlocking the full potential of 6G [10], [11].

The inherent complexity and dynamism of these emerging wireless environments have spurred the adoption of AI algorithms, as conventional optimization methods often lack the agility to cope with rapidly evolving network states and diverse performance criteria. Although learning-based paradigms, such as Deep Learning (DL), have demonstrated potential for specific RAN optimization tasks, their application to multifaceted resource allocation in O-RAN slicing often encounters significant hurdles. These typically include the need for extensive, task-specific agent engineering, computationally intensive training regimens that usually start from scratch, and practical limitations related to sample inefficiency and suboptimal generalization to novel network conditions or previously unseen service demands. Such drawbacks critically hinder the development of truly autonomous systems capable of generating robust, adaptive, and near-optimal resource management strategies in real

time.

The previously discussed limitations of conventional AI methods in achieving adaptable and data-efficient resource allocation for dynamic networks underscore the need for novel Generative Artificial Intelligence (GAI) paradigms. To this end, we propose an innovative GAI framework, termed Generative Semi-Supervised Variational Autoencoder (VAE)-Contrastive Learning (SS-VAE), designed explicitly for intelligent O-RAN network slicing. This framework is realized through a unified architecture that intrinsically integrates the distributional learning and generative capabilities of a VAE [12] with the potent representation learning power of contrastive learning principles [13]. Trained end-to-end using a semi-supervised strategy, our SS-VAE model is designed to learn complex resource distributions and generate optimized allocation decisions with superior generalization and data efficiency.

The synergistic design of our Generative SS-VAE framework offers distinct advantages for GAI-driven resource optimization in O-RAN. The VAE core excels at modeling the underlying probability distributions of network states and resource utilization, which is crucial for managing the inherent uncertainty and can be leveraged to handle incomplete data by inferring missing values from learned patterns. Its generative capability, central to our GAI approach, allows the model to proactively construct or refine resource allocation strategies, finely tuned to diverse QoS demands within O-RAN slices. This is powerfully augmented by the integrated contrastive learning mechanism, which compels the model to learn highly informative and robust latent representations from both limited labeled data and abundant unlabeled data. Such a focus on representation quality, integral to our semi-supervised methodology, significantly enhances sample efficiency and fortifies the model's ability to generalize to unseen network conditions and resist noise or outliers, making it exceptionally suited for the dynamic O-RAN environment.

Our proposed SS-VAE algorithm is designed for practical implementation within the O-RAN architecture. It is envisioned for deployment as an eXtended Application (xApp) operating on the near-real-time Radio Access Network Intelligent Controller (RIC). This strategic placement enables the SS-VAE xApp to dynamically adjust resource allocation by leveraging real-time network telemetry and user demand information, thereby facilitating efficient, adaptive, and QoS-aware management of network slices.

### 1.1 Contribution

This paper makes significant contributions to the field of intelligent resource allocation and network slicing within the O-RAN architecture, explicitly targeting the distinct demands of eMBB and URLLC services. We introduce and rigorously evaluate a novel GAI driven solution. The primary contributions of this work are as follows.

- We present a detailed system model and formulate the resource allocation problem in O-RAN environments, aiming to optimize weighted throughput via efficient assignment of transmission power and PRBs in the downlink. This formulation explicitly considers the unique QoS requirements and service priorities of

eMBB and URLLC services. It is designed for implementation within an xApp-based architecture to enhance the flexibility of AI-driven network management.

- We propose, design and implement a novel GAI framework to optimize resource allocation in O-RAN. This framework employs a unified deep learning architecture that combines a VAE—which captures complex data patterns and can generate resource allocation solutions—with contrastive learning to learn robust and meaningful feature representations. The entire model is trained end-to-end using a semi-supervised approach, which improves both data efficiency and overall performance. This enables effective generalization across various O-RAN environment scenarios. This makes the framework highly adaptable and practical for real-world, dynamic O-RAN systems.
- We demonstrate through extensive simulations and comparative analysis against multiple benchmarks—including the exhaustive search algorithm (ESA) and deep reinforcement learning—that our proposed AI-driven approach achieves near-optimal resource allocation performance with substantially lower computational complexity than state-of-the-art methods. The results validate the robustness, computational efficiency, and scalability of our AI solution, affirming its suitability for real-time resource management in dynamic O-RAN systems. Furthermore, the principles of our semi-supervised generative model pave the way for its application in future multi-vendor O-RAN architectures and evolving service paradigms.

### 1.2 Structure of the Paper

The paper is structured as follows: Section 2 provides a brief overview of the O-RAN architecture and its components relevant to intelligent control. Section 3 reviews related works in resource allocation, particularly focusing on AI-based approaches in O-RAN. In Section 4, we introduce the system model for the resource allocation challenge in the O-RAN architecture and formally define the problem as an optimization task. Section 5 elaborates on our novel Generative AI-driven resource allocation framework, detailing its underlying model architecture and training methodology. Section 6 presents the numerical results from our performance evaluation, comparing our approach against benchmark algorithms. Section 7 provides an analysis of the computational complexity of the employed algorithms. Finally, Section 8 offers concluding remarks and outlines potential future research directions. For clarity, the following section lists the main acronyms used throughout the paper.

### LIST OF ACRONYMS AND ABBREVIATIONS

<b>5G</b>	Fifth Generation
<b>6G</b>	Sixth Generation
<b>AI</b>	Artificial Intelligence
<b>AMF</b>	Access and Mobility Management Function
<b>BS</b>	Base Station
<b>C-RAN</b>	Cloud Radio Access Network
<b>CP</b>	Control Plane

**CSI** Channel State Information  
**CU** Central Unit  
**DL** Deep Learning  
**DM** Diffusion Model  
**DNN** Deep Neural Network  
**DQN** Deep Q-Network  
**DRL** Deep Reinforcement Learning  
**DU** Distributed Unit  
**eMBB** Enhanced Mobile Broadband  
**ESA** Exhaustive Search Algorithm  
**FDRL** Federated Deep Reinforcement Learning  
**FL** Federated Learning  
**GAI** Generative Artificial Intelligence  
**GAN** Generative Adversarial Network  
**KL** Kullback-Leibler  
**LLM** Large Language Model  
**MAC** Medium Access Control  
**MAE** Mean Absolute Error  
**MANO** Management and Orchestration  
**MARL** Multi-Agent Reinforcement Learning  
**MDP** Markov Decision Process  
**MIMO** Multiple-Input Multiple-Output  
**ML** Machine Learning  
**mMTC** Massive Machine-Type Communications  
**MSE** Mean Squared Error  
**near-RT** Near-Real-Time  
**NFV** Network Functions Virtualization  
**NLOS** Non-Line-of-Sight  
**non-RT** Non-Real-Time  
**O-RAN** Open Radio Access Network  
**OPEX** Operational Expenditures  
**PDCP** Packet Data Convergence Protocol  
**PRB** Physical Resource Block  
**QoS** Quality of Service  
**RAN** Radio Access Network  
**RB** Resource Block  
**RIC** Radio Access Network Intelligent Controller  
**RL** Reinforcement Learning  
**RU** Radio Unit  
**SDAP** Service Data Adaptation Protocol  
**SINR** Signal to Interference & Noise Ratio  
**TL** Transfer Learning  
**UE** User Equipment  
**UP** User Plane  
**UPF** User Plane Function  
**URLLC** Ultra-Reliable Low Latency Communications  
**VAE** Variational Autoencoder  
**vRAN** Virtualized Radio Access Network  
**xApp** eXtended Application

## 2 BACKGROUND

The O-RAN Alliance has created an innovative RAN framework designed to enable an open, intelligent, virtualized, and interoperable RAN, which is crucial for affordable, next-generation wireless networks [14]. The O-RAN architecture combines Cloud Radio Access Network (C-RAN) and Virtualized Radio Access Network (vRAN) to create open, interoperable, and flexible mobile networks that support both 5G and future 6G requirements. The core components of O-RAN include the Open Radio Unit (O-RU), the Open

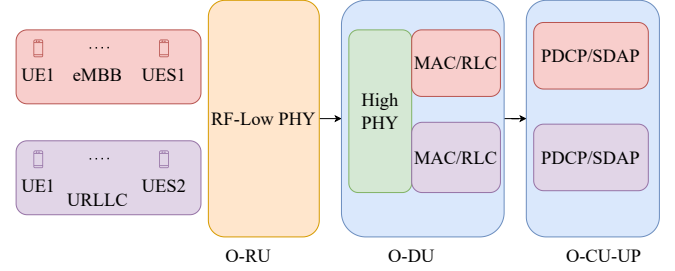


Fig. 1: O-RAN network slicing

Distributed Unit (O-DU), and the Open Centralized Unit (O-CU), each responsible for specific layers of the protocol stack. The O-RU handles radio frequency (RF) and lower physical (PHY) functions. The O-DU processes the medium access control (MAC), radio link control (RLC), and higher PHY layers. Meanwhile, the O-CU manages the Packet Data Convergence Protocol (PDCP) and Service Data Adaptation Protocol (SDAP) and is further divided into the Control Plane (CP) and User Plane (UP) for efficient signaling and traffic routing [14], [15]. Beyond these disaggregated data plane components, key O-RAN architectural pillars include Orchestration and Automation, the O-Cloud, and notably, the RAN RIC. The RIC is pivotal in enabling intelligent network operations, facilitating near-real-time and non-real-time optimization and learning-based control over the RAN.

In the subsequent section, we provide a brief overview of the key methods and characteristics employed in the O-RAN system, which improve its adaptability and efficiency.

### 2.1 Network Slicing in O-RAN

A cornerstone of 5G/6G models, network slicing facilitates the creation of customized virtual networks on demand that operate on shared infrastructure. This end-to-end capability is achieved by logically separating and managing resources across three key domains: the RAN, the core, and the transport network. In the RAN domain, slicing involves partitioning radio resources, such as PRBs, and instantiating dedicated virtual network functions for different services, including MAC/RLC in the O-DU and PDCP/SDAP in the O-CU, as illustrated in Fig. 1. In the core network, key nodes, such as the User Plane Function (UPF) and Access and Mobility Management Function (AMF), are virtualized and isolated to create slices that accommodate specific service-level agreements. The transport network is sliced to create dedicated data pathways, ensuring that the performance and QoS for these diverse connections are guaranteed. The O-RAN framework, with its inherent intelligence and virtualization, serves as a crucial enabler for sophisticated RAN slicing, which is indispensable to perform comprehensive end-to-end network slicing [16], [17].

### 2.2 Radio Intelligent Controller (RIC)

The RIC is functionally divided into two layers: the near-real-time (near-RT) and the non-real-time (non-RT) RIC. The near-RT RIC, designed for control loops operating within 10 milliseconds to 1 second latency, hosts modular xApps

that enable fast and responsive control over RAN functions. These xApps handle tasks such as interference mitigation, handover control, and dynamic resource allocation, interacting with the RAN in real time. They are fundamental to enabling service-level customization, particularly through the use of network slicing. In contrast, the non-RT RIC, typically situated within the broader Orchestration and Automation framework, manages operations with latency requirements exceeding 1 second. It supports functions like policy management, network analytics, and AI model training by hosting rApps. These applications analyze historical data, orchestrate the training of AI models, and generate strategic policies or guidance for the near-RT RIC and its xApps [18], [19].

Together, the non-RT RIC and near-RT RIC establish a hierarchical intelligent control loop. Typically, AI models are trained or designed in the non-RT RIC using historical data and network policies and then deployed or used by xApps in the near-RT RIC for inference and real-time action. This synergy enables predictive and adaptive RAN behavior, significantly enhancing automation in dynamic network environments. Both xApps and rApps are designed to be modular and leverage open interfaces, which encourages third-party innovation and accelerates the deployment of AI-driven functionalities, thereby promoting multi-vendor interoperability within the O-RAN ecosystem.

### 2.3 Artificial Intelligence (AI) in O-RAN

The integration of AI is a foundational tenet of the O-RAN architecture, designed to introduce intelligence and autonomy into network operations. This approach is crucial for enhancing QoS through dynamic optimization and reducing Operational Expenditures (OPEX) through automated management. The application of AI is envisioned across a spectrum of RAN use cases, from real-time resource allocation and traffic steering to anomaly detection and cybersecurity.

To address these challenges, the O-RAN framework is equipped to leverage a diverse range of AI methodologies. Supervised learning enables predictive capabilities, such as traffic forecasting, by training on labeled historical data. In contrast, unsupervised learning identifies latent patterns in unlabeled data for tasks such as user clustering or threat detection. For autonomous control, Reinforcement Learning (RL) and its deep-learning variant (Deep Reinforcement Learning (DRL)) allow agents to derive optimal policies through direct interaction with the network environment. To address privacy concerns in multi-agent environments, Federated Learning (FL) facilitates collaborative model training on distributed data without centralizing sensitive information. Further advancing these capabilities, GAI models like VAEs can learn data distributions to generate synthetic training data or even propose new resource management solutions directly. These core techniques can be augmented by Large Language Models (LLMs), which provides a semantic understanding of unstructured data to enhance the overall intelligence of the system's decision-making.

These AI functionalities are operationally hosted within the O-RAN Intelligent Controllers (RIC). The non-RT RIC typically manages functions with relaxed latency constraints, such as offline model training or acting as the

central server in a Federated Learning setup. Conversely, the near-RT RIC executes tasks requiring rapid response, including model inference for sub-second control loops and the distributed training aspects of RL and FL. This architectural division allows O-RAN to effectively support the entire AI lifecycle, from model creation in the non-RT RIC to real-time deployment and execution in the near-RT RIC.

## 3 RELATED WORKS

As highlighted in Section 1, ensuring reliable connectivity for devices with diverse QoS requirements presents significant challenges for cellular operators, especially in the complex and demanding landscape of 5G and emerging 6G networks [20]. As a result, network slicing has become a key focus of research in cellular networks. With the increasing complexity and diversity of services, methodologies for resource allocation have undergone significant evolution. They have shifted from traditional mathematical optimization and heuristics to more adaptive and intelligent AI-driven approaches [20]–[24].

### 3.1 Conventional Optimization and Heuristic Approaches

Resource allocation in wireless networks has been addressed through formal mathematical optimization and heuristic algorithms [20]–[22], [25]. Algorithms such as Linear and Non-Linear Programming provide a rigorous framework for defining these problems, and for specific cases like convex problems, can even yield globally optimal solutions efficiently. When exact solutions are computationally infeasible due to the NP-hard nature of many practical scenarios involving discrete decisions, a wide range of heuristic and meta-heuristic algorithms, including greedy methods, simulated annealing, and genetic algorithms, have been employed. These methods aim to find good, albeit often suboptimal, solutions quickly, providing a practical alternative to complex optimization.

Despite their utility, these conventional approaches have significant limitations in the context of dynamic, sliced O-RAN environments. Their primary failing is the computational complexity that makes them too slow for the near-real-time control loops required by the O-RAN RIC. Furthermore, these methods typically rely on static models and lack the agility to adapt to the highly dynamic nature of wireless channels, traffic loads, and user mobility. Their performance is tied to the accuracy of underlying network models, and heuristics can be brittle, performing poorly when conditions deviate from their design assumptions. Crucially, they do not learn from operational data to improve future decisions, which makes them ill-suited for the data-rich, learning-driven paradigm enabled by O-RAN's open interfaces.

### 3.2 Discriminative AI and Reinforcement Learning Paradigms

The limitations of conventional optimization have driven research into AI-driven solutions, with DRL emerging as a significant approach for dynamic resource allocation. DRL combines the function approximation capabilities of Deep

Neural Network (DNN) with the trial-and-error framework of RL, enabling agents to learn optimal policies through interaction with their environment. Various DRL algorithms, including value-based methods like Deep Q-Network (DQN) and actor-critic methods such as Soft Actor-Critic, have been utilized in wireless resource management [26]. In complex systems like O-RAN, Multi-Agent Reinforcement Learning (MARL) allows multiple agents to learn simultaneously, optimizing local and global objectives. FL has also gained importance as a distributed machine learning paradigm that facilitates collaborative training without centralizing data, thus preserving privacy. The combination of DRL and FL, termed Federated Deep Reinforcement Learning (FDRL), allows distributed agents to enhance DRL model building. They offer advantages such as adaptability, reduced reliance on precise network models, the ability to manage high-dimensional state spaces, and enhanced data privacy [27]. However, DRL faces challenges such as sample inefficiency, long training times, and poor generalization in new scenarios. Additionally, designing practical reward functions is complex, and the "black box" nature of deep networks raises interpretability concerns. Moreover, FL struggles with non-identically distributed data and communication overhead. DRL effectively learns reactive policies but does not model the generative processes or distributional characteristics of optimal solutions, highlighting the need to explore generative AI approaches to understand these underlying data distributions better.

### 3.3 The Rise of Generative AI in Wireless Network Optimization

A new frontier in AI-driven network optimization is emerging with the application of GAI. Unlike discriminative models that learn decision boundaries or RL agents that learn reactive policies, GAI models are designed to learn the underlying probability distribution of data. This allows them to generate new, synthetic data instances or solutions that exhibit similar characteristics to the training data [28]. The unique capabilities of GAI offer several advantages for complex optimization problems, such as O-RAN resource allocation, including the ability to proactively generate novel and optimized solutions, augment limited training datasets, and robustly model the inherent uncertainty of wireless environments by capturing complex data distributions [29].

This generative capability is realized through several prominent model architectures. VAEs are adept at learning compressed, meaningful representations of high-dimensional network data, making them suitable for both generating solutions and performing inference [1, 49]. Generative Adversarial Networks (GANs) uses a competitive training process and has been primarily explored for data augmentation, creating realistic synthetic channel data or traffic patterns to enhance the robustness of other AI models [35, 45]. More recently, Diffusion Models (DMs) have shown promise for generating high-fidelity samples and are being investigated for imitating expert allocation policies [30]. The choice of model often depends on the specific task, whether it is direct solution generation, data augmentation, or learning latent representations for other processes.

### 3.4 Identifying the Research Gap: Positioning the Proposed SS-VAE Framework

Despite notable advancements, current resource allocation methods in sliced O-RAN environments still face significant challenges. Conventional optimization and heuristic approaches often lack the speed required for real-time control and struggle to adapt to dynamic network conditions. DRL provides adaptability but suffers from poor sample efficiency and limited generalization, as it typically learns reactive policies without fully modeling the optimal solution distribution. Advanced techniques, such as FL and Transfer Learning (TL), offer some benefits but do not adequately address the need to learn from limited labeled data while exploring the vast solution space of NP-hard allocation problems.

There is a pressing need for approaches that can learn robust representations from scarce or mixed-quality data, model complex uncertainties, and explore the solution space in a generative manner to find near-optimal resource allocation strategies. Specifically, this is essential for coordinating multiple xApps within dynamic O-RAN environments. The challenge is heightened by the limited generalizability of existing models across diverse deployment conditions, including varying numbers of User Equipment (UE), fluctuating traffic patterns, and heterogeneous network configurations. This limits their scalability and effectiveness in real-world scenarios.

To address these issues, we propose the Generative Semi-Supervised VAE-Contrastive Learning (SS-VAE) framework, which integrates key AI concepts to fill this gap. At its core, the VAE learns the underlying probability distributions of network states and optimal resource allocations, enabling proactive generation and refinement of allocation decisions. This generative capability is vital for navigating the complex solution landscape of joint resource allocation, moving beyond the reactive tendencies of DRL and the data demands of purely supervised learning. Table 1 summarizes the key characteristics, contributions, and limitations of selected related works alongside the proposed SS-VAE approach.

## 4 SYSTEM MODEL

This study addresses the resource allocation problem in the O-RAN architecture through network slicing, focusing on two primary slice types: URLLC and eMBB. The URLLC slice is designed for ultra-low latency and high-reliability communications, which are essential for critical applications. In contrast, the eMBB slice aims to deliver high data rates for mobile broadband services. Each slice type imposes distinct QoS requirements on resource allocation, as conceptually illustrated for the O-RAN functional split in Fig. 1 [6]. Based on Fig. 1, the O-RU is shared across services. Within the O-DU, the High PHY layer is common, while the MAC and RLC layers are logically separated per slice. In the O-CU-UP, the SDAP and PDCP layers are also sliced to cater to differentiated service needs.

Logically slicing the RAN into separate URLLC and eMBB service-aware components allows for optimized network operation tailored to diverse traffic characteristics, thereby enhancing overall resource efficiency and operational flexibility. Key resources considered for allocation in

TABLE 1: Comparative Analysis of AI-Driven Resource Allocation Methods in O-RAN

Reference	Problem Domain	Methodology	Key Contribution(s)	Limitation(s)	Primary Differentiator vs. This Work
SS-VAE	Multi-resource (power, PRB, UE assoc.) allocation for eMBB/URLLC slicing in O-RAN.	Semi-Supervised Generative AI (VAE with Contrastive Learning).	<ul style="list-style-type: none"> <li>Novel unified GAI framework.</li> <li>Data-efficient via semi-supervision.</li> <li>Generative exploration of solution space.</li> </ul>	Requires initial limited labels from a high-complexity solver.	(Baseline for comparison)
Li et al. [31]	Proactive resource allocation considering UE mobility in HetNets.	DRL.	Adapts proactively to user mobility.	Standard DRL challenges (e.g., sample complexity, generalization).	Learns a reactive policy, whereas our work is generative, learning the solution distribution.
Wu et al. [32]	Joint radio and computation resource allocation for vehicular RAN slicing.	DRL.	Dynamically allocates both radio and compute resources.	Relies on reactive DRL policy; generalization across diverse slice types.	Reactive DRL policy vs. our generative exploration of the joint resource space.
Wang et al. [33]	Resource management for O-RAN RU and DU entities.	Self-Play DRL.	Achieves adaptive decision-making through a self-play paradigm.	Scalability and generalization of self-play in a complex O-RAN environment.	Game-theoretic DRL policy vs. our GAI approach to learning underlying data characteristics.
Ndikumana et al. [34]	Joint task offloading and fronthaul routing in O-RAN to reduce delay.	FL + DRL.	Ensures data privacy via FL while optimizing routing decisions.	High complexity in coordinating FL and DRL; potential convergence issues with non-IID data.	Augments a reactive DRL policy with FL, while our method is a unified generative model.
Mhatre et al. [35]	Efficient resource management in 6G networks.	TL + DRL.	Reduces DRL training overhead by transferring knowledge from related tasks.	TL is task-dependent; still relies on a reactive DRL core.	Aids a reactive policy with TL; our method aims for broader generalization via distributional learning.
Chen & Heydari [36]	Resource governance via adaptive adjustment of network topology.	VAE + DRL.	Optimizes network structure using an RL agent in a VAE-compressed latent space.	High training complexity; uses VAE for state compression, not generation.	VAE is used for state representation for an RL agent; our method is a unified GAI for direct solution generation.
Qiao et al. [37]	Multi-timescale resource allocation for O-RAN slicing (radio & computing).	Parallel Hierarchical DRL.	Decomposes the problem hierarchically to handle complexity and coupled constraints.	High complexity of the hierarchical DRL architecture.	Advanced DRL structure that still learns reactive policies; our method is a single, unified generative model.
Lotfi et al. [26]	Dynamic O-RAN slicing and resource management.	LLM + MARL.	Enriches RL state with semantic context from an LLM for improved planning.	High computational cost of LLMs; relies on the quality of LLM output.	Augments DRL state with LLM semantics; we learn robust features directly from raw data via contrastive learning.
Salama et al. [27]	Resource allocation in O-RAN specifically to support FL processes.	FL + RL + Model-based.	Optimizes O-RAN resources (e.g., power) to improve the efficiency of an ongoing FL task.	Solves a different, specific problem (RA for FL), not a general network slicing problem.	Different problem domains and uses a hybrid of non-generative methods.
Qazzaz et al. [38]	Dynamic PRB allocation in O-RAN based on traffic and QoS.	Supervised ML (Random Forest Classifier).	Provides fast decisions by selecting the best policy from a predefined, finite set of options.	Cannot generate novel allocation policies; the quality of predefined policies bounds performance.	A discriminative model that selects a policy; our model is generative and creates new allocation solutions.

our O-RAN model include transmission power and PRBs. Traffic demands are typically characterized by data rate and bandwidth requirements, while QoS parameters specify the target performance metrics for each service. The overall

system model is depicted in Fig. 2. All variables and parameters used throughout this paper are defined and detailed in Table 2.

In our study, we explore a deployment based on O-RAN,

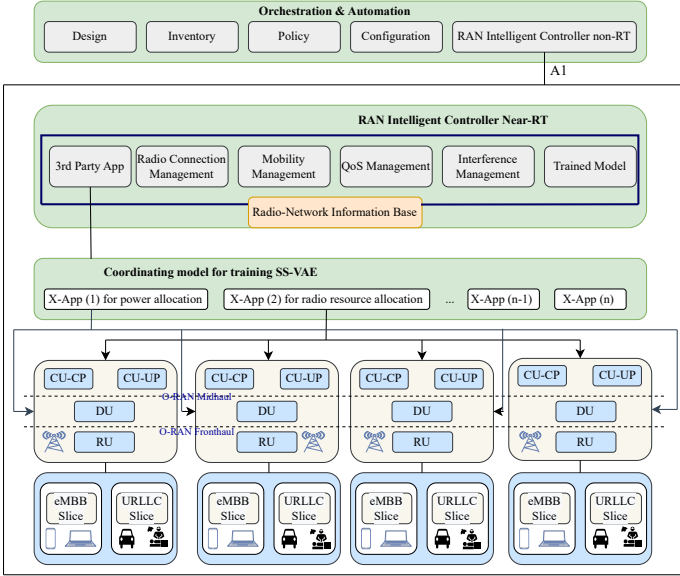


Fig. 2: O-RAN network system model

Notation	Definition
$b, \mathcal{B}, B$	Index, set, and the number of Radio Units (RUs)
$u, \mathcal{U}, U$	Index, set, and the number of UEs
$m, \mathcal{M}, M$	Index, set, and the number of PRBs per RU
$s, \mathcal{S}, S$	Index, set, and the number of slices
$h, \mathcal{H}$	Index, and channel gain matrix between RUs and UEs
$\alpha_{u,s}^b$	UE $u$ association to RU $b$ in slice $s$
$\beta_{u,s,m}^b$	UE $u$ association to PRB $m$ of RU $b$ in slice $s$
$p_{u,s,m}^b$	Transmission power of PRB $m$ of RU $b$ in slice $s$
$R_{u,s,m}^b$	Rate achieved for UE $u$ in PRB $m$ of RU $b$ in slice $s$
$R_{u,s}$	Rate achieved for UE $u$ in slice $s$
$R_u$	Rate achieved for UE $u$
$w_s$	Priority weights for each service type
$P^b$	Transmitted power RU in the fronthaul link
$C^b$	Data rate in the fronthaul link
$\sigma_1^2$	Quantization Noise
$D^{\text{pro}}$	Overall propagation delay
$D^{fr,p}$	Propagation delay in the fronthaul link
$D^{mid,p}$	Propagation delay in the midhaul link
$D^{bc,p}$	Propagation delay in the backhaul link
$L$	Length of the fiber link
$C$	Propagation speed of the medium
$D^{tr}$	Total transmission delay
$D^{fr,t}$	Transmission delay in the fronthaul link
$D^{mid,t}$	Transmission delay in the midhaul link
$D^{bc,t}$	Transmission delay in the backhaul link
$R$	Data rate of the packet
$\mu$	Mean packet size

TABLE 2: Notations with definitions for the system model parameters.

wherein each Base Station (BS), known as RU in O-RAN, supports two different slices: eMBB and URLLC. These slices are designed to meet the QoS requirements of UEs. Our analysis focuses on two key network functions, power control and radio resource allocation, which are jointly considered.

We represent the set of all RUs as  $\mathcal{B}$  and the set of UEs as  $\mathcal{U}$ . Each RU  $b$  serves two sets of UEs:  $\mathcal{U}_e^b$  for eMBB and  $\mathcal{U}_u^b$  for URLLC, leading to a total of  $U$  UEs, where  $U = U_e^b + U_u^b$ . Each UE is exclusively associated with a single RU. The temporal and spectral layout is divided into  $\mathcal{M}$

segments known as PRBs, which are the smallest unit of resources for allocation [39]. Each PRB covers a specific time slot in the temporal domain and a frequency range of  $f$  Hz in the spectral domain. We denote  $S_e$  for eMBB slices and  $S_u$  for URLLC slices.

The UE association is indicated by a binary variable  $\alpha_{u,s}^b$  taking a value of 1 if UE  $u$  in slice  $s$  is connected to RU  $b$  and 0 otherwise. Since each UE should be connected to only one RU, the following constraint must be met:

$$\sum_{b \in \mathcal{B}} \alpha_{u,s}^b = 1, \quad \forall u \in \mathcal{U}, s \in \mathcal{S}. \quad (1)$$

We define the binary variable  $\beta_{u,s,m}^b$  as the indicator for PRB allocation, taking the value of 1 when UE  $u$  in slice  $s$  is connected to PRB  $m$  of RU  $b$ , and 0 otherwise. We have

$$\beta_{u,s,m}^b \leq \alpha_{u,s}^b, \quad \forall b \in \mathcal{B}, m \in \mathcal{M}, u \in \mathcal{U}, s \in \mathcal{S}. \quad (2)$$

Similarly, each PRB  $m$  of RU  $b$  is associated with only one UE, as

$$\sum_{u \in \mathcal{U}} \alpha_{u,s}^b \beta_{u,s,m}^b \leq 1, \quad \forall b \in \mathcal{B}, m \in \mathcal{M}, s \in \mathcal{S}. \quad (3)$$

We denote the transmission power of PRB  $m$  in RU  $b$  in slice  $s$  as  $p_{u,s,m}^b$  for UE  $u$ , and the channel gain between RU  $b$  and UE  $u$  in slice  $s$  as  $h_{u,s,m}^b$ . The rate achieved for UE  $u$  in slice  $s$  by allocating PRB  $m$  of RU  $b$  is denoted by  $R_{u,s,m}^b$ , where  $\eta_{u,s,m}^b$  represents the Signal to Interference & Noise Ratio (SINR). The calculation for  $R_{u,s,m}^b$  is determined by

$$\eta_{u,s,m}^b = \frac{\alpha_{u,s}^b h_{u,s,m}^b p_{u,s,m}^b}{\sum_{j \neq b} \sum_{l \neq s} \sum_{i \neq u} \alpha_{i,l}^j h_{i,l,m}^j p_{i,l,m}^j + \sigma^2}, \quad (4)$$

$$R_{u,s,m}^b = \log_2(1 + \eta_{u,s,m}^b), \quad (5)$$

$$R_{u,s} = \sum_{b \in \mathcal{B}} \sum_{m \in \mathcal{M}} \alpha_{u,s}^b \beta_{u,s,m}^b R_{u,s,m}^b, \quad (6)$$

$$R_u = \sum_{s \in \mathcal{S}} \sum_{u \in \mathcal{U}} \alpha_{u,b,m,s} \sum_{m \in \mathcal{M}} \beta_{u,s,m}^b R_{u,b,m,s} \\ = \sum_{u \in \mathcal{U}} \sum_{m \in \mathcal{M}} \beta_{u,s,m}^b R_{u,s,m}^b \quad \forall m \in \mathcal{M}, s \in \mathcal{S}. \quad (7)$$

The total power transmitted by RU  $b$  and the data rate for UE in the fronthaul link are represented as  $P^b$  and  $C^b$ , respectively. Quantization noise ( $\sigma_1^2$ ) can potentially impact the signal's fidelity during transmission over the fronthaul, mainly when the original signal displays significant variations or spans a wide range of values. This noise may lead to inaccuracies in the transmitted signal, thereby influencing the QoS perceived by the UE. These values are determined as follows:

$$P^b = \sum_{u=1}^U \sum_{m=1}^M \sum_{s=1}^S \alpha_{u,s}^b h_{u,s,m}^b p_{u,s,m}^b + \sigma_1^2, \quad (8)$$

$$C^b = \log_2\left(1 + \frac{\sum_{u=1}^U \sum_{m=1}^M \sum_{s=1}^S \alpha_{u,s}^b h_{u,s,m}^b p_{u,s,m}^b}{\sigma_1^2}\right) \\ = \log_2\left(\frac{P_b}{\sigma_1^2}\right). \quad (9)$$

The channel characteristics in our model are simulated using a Rayleigh fading process, which represents the variable channel conditions typical of non-line-of-sight (NLOS) environments. The channel vector from PRB  $m$  in RU



$b$  to  $u$  UE in  $s$  slice, denoted by  $\mathbf{h}_{u_s,m}^b$ , is modeled as  $\mathbf{h}_{u_s,m}^b = \sqrt{\beta_{u_s,m}^b} \mathbf{g}_{u_s,m}^b$ , where  $\beta_{u_s,m}^b$  represents the large-scale fading coefficient, accounting for path loss and shadowing, and  $\mathbf{g}_{u_s,m}^b \sim \mathcal{N}(0, N_0 I_{D_s})$  is the fast and flat fading effects modeled as a circularly symmetric complex Gaussian random variable. To reflect the impact of interference and uncertainties, the channel gain matrix  $\mathbf{H}$  is augmented with Gaussian noise, expressed as  $\mathbf{H}_{noise} = \mathbf{H} + \epsilon$ , where  $\epsilon$  is a Gaussian noise matrix with zero mean and adjustable variance  $\sigma^2$ .

The total delay experienced by each UE is the sum of propagation and transmission delays. The overall propagation delay ( $D^{pro}$ ) consists of the delays in the fronthaul ( $D^{fr,p}$ ), midhaul ( $D^{mid,p}$ ), and backhaul ( $D^{bc,p}$ ) links. In each of these links, the propagation delay is determined as the time it takes for a signal to traverse the distance, calculated as  $D = L/C$ , where  $L$  is the link length and  $C$  is the propagation speed. Similarly, the total transmission delay ( $D^{tr}$ ) is the sum of transmission delays in the fronthaul ( $D^{fr,t}$ ), midhaul ( $D^{mid,t}$ ), and backhaul ( $D^{bc,t}$ ) links. Within each link, the transmission delay corresponds to the time needed to transmit all packets into the transmission medium, determined by  $D = \frac{\mu}{R_{u_s}}$ , where  $R_{u_s}$  is the data rate for UE  $u$  in slice  $s$ , and  $\mu$  is the mean packet size. The total delay for UE  $u$  in slice  $s$  is  $D_{u_s} = L/C + \mu/R_{u_s}$ , and should be below a specific threshold ( $D_{u_s}^{max}$ ), expressed as  $D_{u_s} \leq D_{u_s}^{max}$ .

The objective of our resource allocation scheme is to optimize the overall network utility. This primarily involves maximizing the weighted sum of the data rates,  $R_{u_s}$ , achieved by all UEs, while simultaneously satisfying their respective QoS requirements, particularly the delay constraints. The weight  $w_s$  reflects the priority or importance associated with service type  $s$  (e.g., eMBB or URLLC). The intelligent resource allocation function, managed by xApps at the RIC and influencing RU behavior, is responsible for effectively managing these diverse requirements. Hence, we can mathematically express the optimization problem as follows:

$$\max_{\mathbf{p}, \alpha, \beta} \sum_{s \in \mathcal{S}} \sum_{u \in \mathcal{U}} w_s R_{u_s} \quad (10)$$

subject to

$$P^b \leq P_b^{max} \quad \forall b \in \mathcal{B} \quad (11)$$

$$p_{u_s,m}^b \geq 0 \quad \forall b \in \mathcal{B}, m \in \mathcal{M}, s \in \mathcal{S}, u \in \mathcal{U} \quad (12)$$

$$p_{u_s,m}^b \leq P_s^{max} \quad \forall b \in \mathcal{B}, m \in \mathcal{M}, s \in \mathcal{S}, u \in \mathcal{U} \quad (13)$$

$$R_{u_s} \geq R_s^{min} \quad \forall u \in \mathcal{U}, s \in \mathcal{S} \quad (14)$$

$$C^b \leq C_b^{max} \quad \forall b \in \mathcal{B} \quad (15)$$

$$D_{u_s} \leq D_{u_s}^{max} \quad \forall u \in \mathcal{U}, s \in \mathcal{S} \quad (16)$$

$$\alpha_{u_s}^b \in \{0, 1\} \quad \forall u \in \mathcal{U}, b \in \mathcal{B}, s \in \mathcal{S} \quad (17)$$

$$\beta_{u_s,m}^b \in \{0, 1\} \quad \forall u \in \mathcal{U}, b \in \mathcal{B}, m \in \mathcal{M}, s \in \mathcal{S} \quad (18)$$

$$\sum_{b \in \mathcal{B}} \alpha_{u_s}^b = 1 \quad \forall u \in \mathcal{U}, s \in \mathcal{S} \quad (19)$$

$$\beta_{u_s,m}^b \leq \alpha_{u_s}^b \quad \forall b \in \mathcal{B}, m \in \mathcal{M}, u \in \mathcal{U}, s \in \mathcal{S} \quad (20)$$

$$\sum_{u \in \mathcal{U}} \alpha_{u_s}^b \beta_{u_s,m}^b \leq 1 \quad \forall b \in \mathcal{B}, m \in \mathcal{M}, s \in \mathcal{S} \quad (21)$$

Equation (10) defines the objective of maximizing the total weighted data rate across all users and services. Constraints (11), (12), and (13) enforce limitations on the transmit power for each RU, ensure non-negative power allocation for each UE, and restrict the received power per UE, respectively.

Constraint (14) guarantees the QoS by ensuring that each service meets its minimum required data rate. Furthermore, (15) and (16) account for the fronthaul capacity limitations of each RU and the delay constraints for each UE, respectively, by their QoS requirements.

Constraints (17) and (18) define the binary nature of the decision variables  $\alpha$  and  $\beta$ . Finally, constraints (19), (20), and (21) ensure that each UE is associated with exactly one RU and that Resource Block (RB) assignments are only made if the UE is associated with the corresponding RU while preventing multiple UEs from sharing the same RB on the same RU.

This formulation can be seen as a well-known NP-hard problem, a multi-dimensional knapsack problem. Since we can reduce it to our resource allocation problem in polynomial time, it follows that it is also NP-hard. Given the NP-hard nature of the resource allocation problem, finding an exact solution in polynomial time is computationally infeasible for large-scale networks.

The system model is constrained by limited resources, such as UE or RU, and slice power and fronthaul capacity, which prevents the aggregate throughput from exceeding its optimal value. This ensures that the objective function, representing aggregate throughput, has an upper bound and cannot increase infinitely. As a result, the algorithm used to solve the system will converge to an optimal solution. If the objective function is a strictly increasing function concerning the number of iterations, it will converge to its global optimum. The algorithm will converge to a local optimum if the function is non-monotonically ascending. This guarantees the stability and convergence of the system model within the feasible region.

## 5 METHODOLOGY

To address the complex resource allocation problem in the O-RAN architecture, we introduce SS-VAE, a novel GAI framework rooted in semi-supervised learning. This method employs a specialized DNN architecture that intrinsically integrates a VAE—leveraging its ability to learn underlying data distributions—with a contrastive loss function designed to enhance representation quality. The SS-VAE is designed to comprehend complex relationships between input features and optimal resource allocation decisions (e.g., parameters  $\alpha$ ,  $\beta$ , and transmission powers) that meet stringent QoS requirements. A comprehensive dataset underpins the development and initial supervised training of SS-VAE. This dataset features diverse O-RAN scenarios, with labeled data representing optimal allocation parameters generated via an Exhaustive Search Algorithm (ESA), which also serves as an optimal performance benchmark.



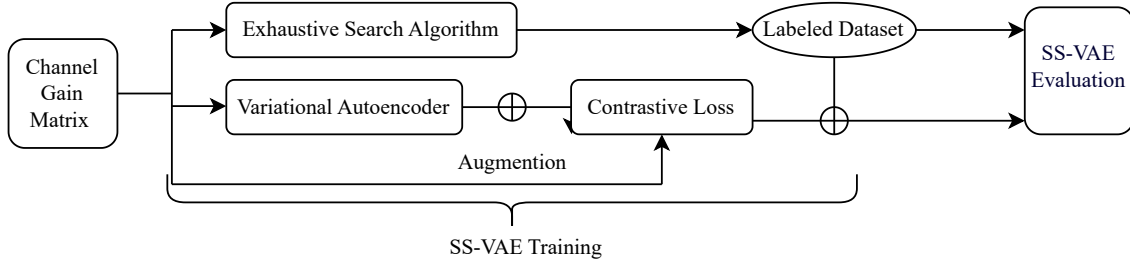


Fig. 3: Overview of the proposed methodology.

The robustness and efficacy of the SS-VAE framework will be rigorously evaluated using multiple regression-based metrics suitable for assessing the accuracy of the generated resource allocation parameters. Its performance will be benchmarked against both the globally optimal solutions derived from ESA and deployment-ready, state-of-the-art methods such as DRL agents. This comprehensive validation aims to demonstrate the reliability of SS-VAE across various operational scenarios, particularly highlighting its capability to approach optimal performance without the prohibitive computational cost associated with ESA. Fig. 3 illustrates our proposed methodology, which encompasses the training pipeline for SS-VAE and a comparative evaluation against benchmark algorithms.

### 5.1 Exhaustive Search Algorithm (ESA)

We employ ESA method as a basis of comparison for our algorithm. The ESA is a fundamental method to find the global optimal solution for resource allocation problems by exhaustively evaluating all possible configurations based on a predefined objective function [40]. It serves as a benchmark by providing a ground truth for comparing other methods. While it is simple to understand and guarantees optimality within a finite time, its high computational cost limits its use to small or well-defined problems [41]. Nevertheless, it remains a widely used benchmark for evaluating and comparing optimization algorithms.

We use the ESA to create a labeled dataset by obtaining a subset of optimal solutions for the objective variables (i.e.,  $\alpha$ ,  $\beta$ ,  $p$ ) in the resource allocation optimization problem. This dataset is subsequently used to train the supervised learning component of our SS-VAE method. The detailed steps of the ESA are described in Algorithm 1.

### 5.2 Deep Reinforcement learning Algorithm

To evaluate the proposed SS-VAE methodology, we benchmark its performance against a DRL model, a paradigm increasingly recognized for its efficacy in navigating complex resource allocation tasks within contemporary wireless networks [42]. The resource allocation challenge, as formulated in Problem 10, is cast as a Markov Decision Process (MDP). This formalization allows the O-RAN orchestrator, responsible for PRB assignments and RU associations per slice, to operate as a learning agent [42]–[45]. The MDP is characterized by:

- I. **State:** The state at time  $t$  ( $\mathbf{s}(t) \in \mathcal{S}$ ), is represented by  $\{\mathbf{s}_u(t)\}_{t=1}^N$ , where  $\mathbf{s}_u(t)$  indicates the state of UE  $u$

---

#### Algorithm 1 ESA for Resource Allocation in O-RAN

---

**Require:**  $B, U, S, M, w_s, P_b^{max}, P_s^{max}, R_s^{min}, C_b^{max}, D_{u,s}^{min}$ , and  $H$

**Ensure:** Optimal resource allocation  $best\_solution$  and its objective value  $best\_value$

- 1: Initialize dataset  $\mathcal{X} \leftarrow \emptyset$
  - 2:  $best\_value \leftarrow -\infty$
  - 3:  $best\_solution \leftarrow \emptyset$
  - 4: **for** each possible combination of  $(\alpha, \beta, p)$  **do**
  - 5:   Calculate  $R_{u,s}$  using Eq. (7)
  - 6:   **if** all constraints are satisfied **then**
  - 7:      $current\_value \leftarrow \sum_{s \in S} \sum_{u \in U} w_s R_{u,s}$
  - 8:     **if**  $current\_value > best\_value$  **then**
  - 9:        $best\_value \leftarrow current\_value$
  - 10:        $best\_solution \leftarrow (\alpha, \beta, p)$
  - 11:       Add  $(\alpha, \beta, p, R_{u,s})$  to dataset  $\mathcal{X}$
  - 12:   **end if**
  - 13: **end for**
  - 14: **return**  $best\_solution, best\_value, \mathcal{X}$
- 

( $u = 1 : U$ ). Here,  $\mathbf{s}_u(t)$  is a binary indicator: it equals one if the data rate requirement of UE  $u$  is satisfied and 0 otherwise. Each data rate also corresponds to a quantized transmission power level.

- II. **Action:** An action ( $\mathbf{a} \in \mathcal{A}$ ), is represented as  $\mathbf{a} = \{\alpha_{u,b,s}, \{\beta_{u,b,m,s}\}_{m=1}^M\}_{b=1}^B$ .
- III. **Transition Probability:** The transition probability  $\mathcal{P}(\mathbf{s}'|\mathbf{s}, \mathbf{a})$  represents the probability of moving from one state  $\mathbf{s}$  to another one  $\mathbf{s}'$  by taking action  $\mathbf{a}$ . It is influenced by several factors, including the QoS requirements of UEs and the resource allocation decisions made for UEs.
- IV. **Reward:** The reward function evaluates the gains or costs of a given state-action pair. It guides the agent's decision-making process by indicating the desirability of various actions across different states. Consistent with previous studies [42]–[44], our approach defines the reward function as a combination of the objective function and the constraints pertinent to the considered problem (Equation 10). Thus, we specify the reward function for our specific scenario as follows:

$$\mathcal{R}(\mathbf{s}, \mathbf{a}) = \Theta_r R_{u,s} + \Theta_{const.} C_{u,s,m}^b + \Theta_{bias}, \quad (22)$$

where,  $\Theta_r$ ,  $\Theta_{const.}$ , and  $\Theta_{bias}$  represent the respective weights assigned to the objective function (Data Rate),

constraints, and the bias value. The primary objective of the agent is to determine the optimal policy, denoted as  $\pi : \mathcal{S} \rightarrow \mathcal{P}(\mathcal{A})$ , for the MDP, that maximizes the cumulative reward obtained through dynamic learning from acquired data.

The inherent complexity of wireless resource allocation, characterized by high-dimensional state and action spaces and continuous variables (e.g., transmission power), renders traditional Q-learning approaches inefficient due to the curse of dimensionality and issues with generalizing from sparsely visited state-action pairs [42], [45]. We employ a DQN framework to surmount these challenges. DQN leverages a DNN to approximate the action-value function (Q-function), enabling it to manage large-scale problems effectively. Crucially, DQN incorporates mechanisms such as experience replay—storing transitions  $(\mathcal{S}_t, \mathcal{A}_t, \mathcal{R}_t, \mathcal{S}_{t+1})$  in a replay memory ( $\mathcal{M}$ ) to break data correlations—and target networks to stabilize the learning process and improve convergence.

To ensure a robust exploration-exploitation balance during training, the DQN agent utilizes an epsilon-greedy strategy for action selection:

$$\pi(S) = \begin{cases} \operatorname{argmax}_a Q(\mathcal{S}, a) & \text{with probability } 1 - \epsilon \\ \text{random action} & \text{with probability } \epsilon \end{cases}$$

This allows the agent to exploit its current knowledge by selecting the action with the highest estimated Q-value with probability  $(1 - \epsilon)$  or to explore the action space randomly with probability  $(\epsilon)$ . The comprehensive training algorithm for the DQN is detailed, and our specific implementation for this problem is encapsulated in Algorithm 3 [45].

### 5.3 Semi-Supervised VAE (SS-VAE)

To address the resource allocation problem, we introduce our SS-VAE method in this subsection. The model is designed to process a flattened channel gain matrix (dimension  $U \times B$ ) through a DNN to find optimal resource allocation strategies. The central contribution of our method is the integration of a VAE with a contrastive loss, which improves the learning of refined representations..

In our framework, xApps for power transmission and PRB allocation coordinate through a shared VAE foundation. This VAE acts as a common space, allowing xApps to collaboratively consider relevant features by accessing a shared latent representation of channel gain matrices. This shared understanding facilitates a cohesive analysis and simultaneous consideration of key features impacting both domains. This leads to more comprehensive and informed resource allocation decisions and enables synchronized O-RAN resource management.

#### 5.3.1 Variational Autoencoder

The VAE, a DNN generative model for unsupervised learning, excels at capturing the intrinsic distribution of input data like the channel gain matrix, which is valuable for the resource allocation problem [46]. It maps input data  $x$  (flattened channel gain matrix) to a lower-dimensional latent space  $z$ , with  $p_\theta(z|x)$  as the generative model. The VAE

aims to maximize data likelihood given model parameters  $\theta$ , as expressed mathematically by:

$$\log p_\theta(x) = \mathbb{E}_{q_\phi(z|x)} [\log p_\theta(x|z)] - D_{KL}(q_\phi(z|x)|p(z)), \quad (23)$$

where  $q_\phi(z|x)$  is the encoder to model the posterior distribution of the latent variable based on the input data, and  $D_{KL}(q_\phi(z|x)|p(z))$ , is the Kullback-Leibler (KL) divergence this posterior distribution and the prior distribution of the latent variable. Optimizing the loss (Equation 23) involves adjusting generative model ( $\theta$ ) and encoder ( $\phi$ ) parameters [46]. As illustrated in Fig. 4, the VAE's encoder compresses the channel gain matrix into a lower-dimensional latent code, and the decoder reconstructs it, minimizing reconstruction loss during training.

Using VAEs for resource allocation offers advantages like representing complex distributions, capturing non-linear relationships, and providing a compressed latent space useful for other tasks. They offer a versatile solution to inherently non-convex and challenging resource allocation problems.

The dataset used to train the SS-VAE model consists of  $Q$  training samples, divided into two categories:  $Q_L$  labeled samples and  $Q_U$  unlabeled samples. These samples are represented by pairs of channel matrices and their corresponding power allocation vectors, denoted as  $H_i$  and  $\Gamma_i$  for labeled samples (where  $i$  ranges from 1 to  $Q_L$ ), and  $H_j$  for unlabeled samples (where  $j$  ranges from 1 to  $Q_U$ ). The labeled dataset results from the ESA applied to the same training dataset. Specifically, we have used power transmission and allocation decisions  $(p, \alpha, \beta)$  obtained by ESA as labels for training our SS-VAE model. The supervised learning component of our algorithm uses the ADAM [47] optimizer and an Mean Squared Error (MSE) loss function for the  $Q_L$  labeled samples, defined as follows:

$$L_{supervised} = \frac{1}{\beta_L} \sum_{i \in \beta_L} ||\text{encoder}(\text{VAE}(H_i)) - \Gamma_i||^2. \quad (24)$$

The encoder part of the VAE is used to estimate the transmission power and predict the allocation indicators  $(\alpha_{u_s}^b$  and  $\beta_{u_s, m}^b)$  from the flattened  $UB$  dimensional input channel gain matrix.

#### 5.3.2 Contrastive Loss

Contrastive loss, common in DL for representation learning, aims to map similar data points closer and dissimilar ones further apart in the representation space [13]. Mathematically, it can be expressed as:

$$L = \frac{1}{2N} \sum_{i=1}^N (y_i \cdot d^2(\mathbf{x}_i, \mathbf{x}_i^+) + (1 - y_i) \cdot \max(0, m - d^2(\mathbf{x}_i, \mathbf{x}_i^-))), \quad (25)$$

where  $N$  is the number of data points,  $\mathbf{x}_i$  is the  $i^{th}$  data point,  $\mathbf{x}_i^+$  and  $\mathbf{x}_i^-$  are similar and dissimilar data points,  $y_i$  is a binary label indicating whether  $\mathbf{x}_i$  and  $\mathbf{x}_i^+$  are similar or dissimilar,  $d(\mathbf{x}_i, \mathbf{x}_i^+)$  is the distance function between  $\mathbf{x}_i$  and  $\mathbf{x}_i^+$ , and  $m$  is a margin that separates the similar and dissimilar data points.

To apply contrastive loss in our resource allocation problem, we generate similar and dissimilar channel gain

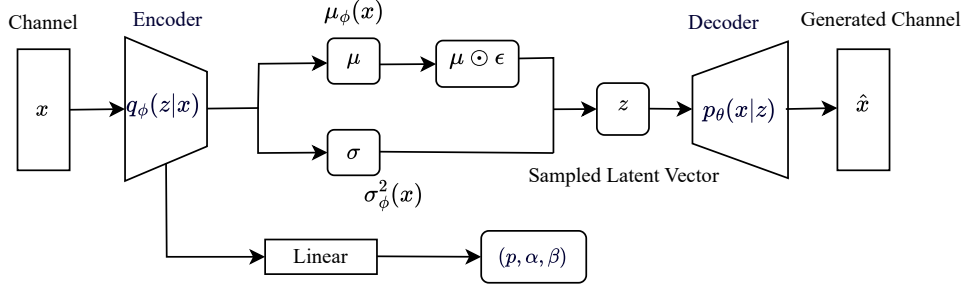


Fig. 4: Architecture of the VAE.

matrices using a channel statistical model that captures the communication environment. Introducing randomness via a Rayleigh fading model produces matrices with varying magnitude and phase coefficients. Specifically, we create a complex Gaussian random matrix with zero mean, where the variance depends on transmitter-receiver distance and accounts for interference as noise [48], [49]. Adjusting this variance controls channel correlation, creating similar or dissimilar matrices. With these, we train our model using the contrastive loss function formulated as follows:

$$L_{Contrastive}(\theta) = \frac{1}{\beta_L} \sum_{i \in \beta_L} \left[ -\log \frac{\exp \frac{f(\underline{H}_i)^T \times f(\underline{H}_i)}{\tau}}{\exp \frac{f(\underline{H}_i)^T \times f(\underline{H}_i)}{\tau} + \sum_{i \neq j} \exp \frac{f(\underline{H}_i)^T \times f(\underline{H}_j)}{\tau}} \right], \quad (26)$$

where  $\theta$  is the set of parameters in the VAE model,  $\tau$  is a temperature hyperparameter, and  $L(\theta)$  is the contrastive loss function.  $\underline{H}_i$  and  $\bar{H}_i$  are matrices similar to the main channel gain matrix  $H_i$ , used for training the SS-VAE model [50]. Minimizing this loss finds  $\theta$  that enables the model to distinguish similar and dissimilar channel gain matrices, thereby addressing the resource allocation problem. The connection between the VAE and the contrastive loss is key for optimal performance. The first step uses supervised learning to learn a good representation of the problem, and the next step refines these representations, improving the model's generalization to new, unseen scenarios.

### 5.3.3 Training the SS-VAE model

The SS-VAE training consists of two parts: supervised learning (i.e., training the VAE using its encoder for prediction) and unsupervised learning (i.e., utilizing contrastive loss to enhance generalization and robustness). Key hyperparameters include the latent space dimension (balancing expressiveness and overfitting) [51], learning rate, batch size, and the number of epochs.  $L1$  and  $L2$  regularization mitigates overfitting [52]. The model uses PyTorch [53], with a 20% validation/test split. Tuned hyperparameters are in Table 5.

### 5.3.4 Performance Metrics

The performance metrics for evaluating our approach include Mean Absolute Error (MAE) ( $MAE = 1/N \sum_{i=1}^N |y_i - \hat{y}_i|$ ), cosine similarity ( $\text{Cosine-Similarity}(Y, \hat{Y}) = Y \cdot \hat{Y} / (|Y| |\hat{Y}|)$ ), and Pearson correlation ( $\text{correlation}(\hat{Y}, Y) = \text{cov}(\hat{Y}, Y) / (\sigma_{\hat{Y}} \sigma_Y)$ ). Here,  $N$  is the total number of samples,

$y_i$  and  $\hat{y}_i$  represent the true and predicted values, the dot product is denoted by  $\cdot$ , and vector magnitude by  $|\cdot|$ . The covariance between predicted and actual values is  $\text{cov}(\hat{Y}, Y)$ , with  $\sigma_{\hat{Y}}$  and  $\sigma_Y$  as their standard deviations.

## 6 SIMULATION RESULTS

We analyzed the initial values in the following subsections to simulate the SS-VAE algorithm. Subsequently, we will compare the results obtained using SS-VAE with those from ESA and DQN.

### 6.1 Simulation Configuration

This section presents the numerical results for the resource allocation problem to evaluate the performance of the SS-VAE model compared to ESA and DQN. In our training and testing scenarios, each RU in the O-RAN deployment is equipped with 25 PRBs and operates with a single antenna with 10 UEs for each service. We consider a network with two slices/services, eMBB and URLLC services. These UEs are randomly distributed within a single-cell environment, mostly 10 to 500 meters from the RU. The initial values and parameters used to run and simulate SS-VAE and the benchmark algorithms (ESA and DQN) are provided in Table 3, Table 4, and Table 5.

For traffic generation, URLLC packets follow a constant bit rate (CBR) model with small fixed payloads of 32 bytes transmitted every 1 ms, resulting in a data rate of approximately 256 kbps per URLLC user. In contrast, eMBB traffic is modeled using a Poisson arrival process with packets sized at 1000 bytes to emulate realistic bursty user behavior such as web browsing and file downloads.

For the channel modeling, we adopt the standard 3GPP-compliant formulation where the channel coefficient between user  $u_s$  and RU  $b$  on PRB  $m$  is given by  $h_{u_s, m}^b = \sqrt{\beta_{u_s, m}^b} \mathbf{g}_{u_s, m}^b$ . The large-scale fading component  $\beta_{u_s, m}^b$  accounts for both path loss and shadowing and is computed as  $\beta_{u_s, m}^b = 10^{-(\text{PL}_{\text{dB}} + S)/10}$ , where the path loss in dB is modeled using the 3GPP Urban Macro (UMa) path loss model which is formulated as  $\text{PL}_{\text{dB}} = 13.54 + 39.08 \log_{10}(d) + 20 \log_{10}(f_c)$ , where  $d$  is the 2D distance between the UE and RU in meters, and  $f_c$  is the carrier frequency in GHz. For  $f_c = 2$  GHz, this simplifies to  $\text{PL}_{\text{dB}} = 13.54 + 39.08 \log_{10}(d) + 6.02$ . Shadow fading  $S$  follows a log-normal distribution  $\mathcal{N}(0, 8^2)$ .

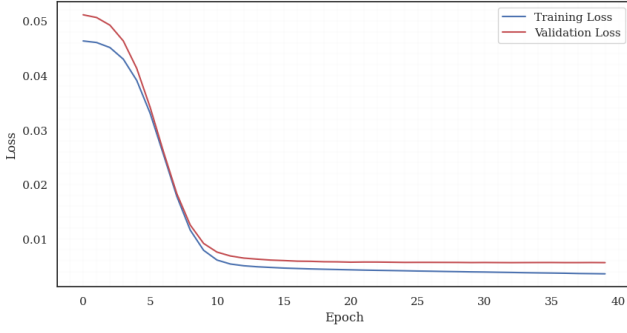


Fig. 5: Loss values of training and validation dataset.

The small-scale fading component  $\mathbf{g}_{u_s, m}^b$  is modeled as a Rayleigh fading coefficient, i.e.,  $\mathbf{g}_{u_s, m}^b \sim \mathcal{CN}(0, 1)$ , to represent non-line-of-sight propagation conditions.

## 6.2 Performance of Model Training

This section describes the performance of the trained model. Fig. 5 shows the training and validation loss values. The decreasing trend of loss values indicates that the SS-VAE method could accurately estimate the target values (power of transmission, association indicators). The model can map the input channel gain matrix to the power of transmission and the indicators by employing the encoder part of the VAE to learn the underlying information.

The performance metrics for the test data, as given in Table 6, clearly indicate that the SS-VAE method obtained optimal performance in the test dataset, demonstrating its generalization ability. The  $R_{Score}^2$  value for the test data indicates that our model successfully explains a significant portion of the variance in estimating the power of transmissions. This improvement can be attributed to the utilization of VAE, which has been proven to enhance generalization in various related tasks. Furthermore, the pre-training method involving contrastive loss has improved our model's ability to learn the underlying features, reducing generalization errors.

## 6.3 Comparison of the Algorithms

We evaluated the performance of our SS-VAE method compared to the ESA algorithm, focusing on how the number of labeled samples used for training affects the results, as shown in Fig. 6a. We analyze the aggregated throughput under varying numbers of labeled data points obtained by the SS-VAE algorithm and the ESA. As depicted in Fig. 6a, SS-VAE achieves a similar aggregated throughput compared to the ESA. Moreover, the discrepancy between SS-VAE and the ESA decreases significantly as the number of labeled data points increases. The difference in aggregated throughput between these methods is 2.1 for 2000 labeled samples, which will be decreased using more labeled samples.

We also evaluate the performance of the SS-VAE and ESA based on binary variables related to user association ( $\alpha_{u_s}^b$ ) and PRB allocation ( $\beta_{u_s, m}^b$ ). Fig. 6b displays the ratio of the absolute sum of differences in these binary variables between the SS-VAE and ESA to the total number of them ( $|\alpha_{ESA} - \alpha_{SS-VAE}| + |\beta_{ESA} -$

$\beta_{SS-VAE}|$ )/# Number of ( $\alpha$ & $\beta$ ), as the number of labeled samples increases. The difference between them reaches its minimum at 2000 samples (4.7% error) and is expected to decrease significantly as more labeled samples are used.

These results demonstrate the reliable performance of our SS-VAE method in addressing the resource allocation problem. The following section will evaluate its performance under varying initial conditions, including different slice numbers, UEs, and transmission power and rate thresholds. Although SS-VAE shows lower error than ESA, it does not perform identically in resource allocation. Therefore, we will also compare it with the DQN algorithm, which has shown effective results in similar resource allocation problems within wireless networks [42], [54], [55].

## 6.4 Performance Results

Fig. 6c demonstrates the aggregated throughput obtained by SS-VAE, ESA, and DQN for different number of UEs. The difference in performance between SS-VAE and ESA is consistent across all UEs. Moreover, ESA achieves higher aggregate throughput than SS-VAE, outperforming DQN in total throughput across all UEs. In addition, the aggregated throughput increases initially as more UEs join the service for all three examined algorithms. However, it reaches a plateau after 30-35 UEs per service due to power limitations and interference constraints. Fig. 6d shows the aggregated throughput achieved by the SS-VAE algorithm at different maximum power levels of O-RU and different numbers of UEs. In resonance with [17], increasing the maximum power of O-RU and the number of UEs leads to higher aggregated throughput. The highest aggregated throughput is observed when the maximum power of O-RU is at its highest.

Figures 6e and 6f show the aggregated throughput for two service types—eMBB and URLLC—obtained using the SS-VAE and DQN algorithms. Specifically, Fig. 6e illustrates the weighted aggregate throughput as a function of the maximum power of the RU, while Fig. 6f presents the throughput variation concerning the maximum power allocated per slice. Both figures compare the performance of SS-VAE and DQN across different power constraints for these services. They demonstrate a direct correlation between increased maximum power levels and higher weighted throughput. Across all scenarios, the SS-VAE algorithm consistently outperforms the DQN algorithm, providing higher aggregate throughput for both service types, regardless of whether the power levels pertain to the RU or the individual slices. Due to their need for higher data rates, eMBB service type exhibits higher aggregate throughput than URLLC services. This consistent performance advantage underscores the effectiveness of the SS-VAE algorithm in optimizing resource allocation across different power settings.

Although ESA ensures a globally optimal solution, its computational complexity makes it impractical for real-world applications. DQN, while powerful, faces challenges related to convergence time, exploration efficiency, and sample requirements. Our SS-VAE method employs the strengths of supervised and unsupervised learning to provide a scalable and efficient solution for resource allocation in O-RAN, outperforming these benchmarks in real-world

TABLE 3: Resource Allocation Simulation Parameters

Parameter	Value
Noise power	-174 dBm
bandwidth of each sub-carrier	180 KHz
Maximum transmit power of each O-RU	40 dBm
Maximum fronthaul capacity	46 bps/Hz
Maximum data rate for eMBB	10 bps/Hz
Maximum data rate for URLLC	2 bps/Hz
Maximum power for URLLC & eMBB	30 dBm

TABLE 4: DQN Training Parameters

Number of episodes and steps	250, 50
$\gamma, \epsilon_{\text{final value}}, \epsilon_{\text{decay factor}}$	0.9, 0.1, 0.9995
Replay memory size	400

TABLE 6: Performance metrics of the SS-VAE model

Performance Metric	MAE	$R_{\text{Score}}^2$	Cosine Similarity
Value	0.09207532	0.76795106	0.988023

scenarios. This contrasts with DQN, which may struggle with generalization due to its reliance on extensive exploration and sample efficiency. Additionally, DQN often requires significant training time to converge to an optimal solution, especially in environments with high variability and complex constraints. It may also face challenges with exploration efficiency, often requiring many iterations to fully explore the solution space, which can result in sub-optimal performance under dynamic conditions.

## 7 COMPUTATIONAL COMPLEXITY ANALYSIS

This section analyzes the computational costs of the ESA, DQN, and the SS-VAE method and discusses how each algorithm scales with increasing network size and complexity.

### 7.0.1 ESA

The ESA evaluates all possible combinations of resource allocations to find the global optimal solution. If there are  $|U|$  UEs,  $|B|$  RUs,  $M$  PRBs, and  $P_{\text{levels}}$  number of discrete power levels, the total cost is given by:

$$\text{Total Cost} = (|B|^{|U|}) \times \prod_b (\sum_s \sum_u \alpha_{u,s}^b + 1)^M \times P_{\text{levels}}$$

Where  $\prod_b (\sum_s \sum_u \alpha_{u,s}^b + 1)^M$  represents the worst case number of possible PRB assignments to UEs without intra-cell interference in each RU  $b$ , ESA needs to scale better with increasing network size and complexity due to its exponential growth in computational requirements. Despite its guarantee of finding the global optimal solution, it is impractical for real-time applications and large-scale networks.

### 7.0.2 DQN

The complexity of training a DQN is expressed as  $O(E \cdot (T \cdot (|S| \cdot |A| + F)))$ , where  $E$  is the number of episodes,  $T$  is the number of steps per episode,  $|S|$  is the size of the state space,  $|A|$  is the size of the action space, and  $F$  denotes the complexity of the neural network forward pass and backpropagation. The complexity of making a decision using a trained DQN is  $O(F)$ , where  $F$  is the neural network forward pass complexity. The total computational cost for

TABLE 5: SS-VAE Model Training Parameters

Type	Training Parameter	Value
Optimizer	Initial learning rate	0.001
	$\beta_1$	0.99
	$\beta_2$	0.99
	Weight Decay	0.9
Model	Number of encoding layer	20
	Dimension of latent space	20
	Contrastive loss temperature	0.25
	Activation Function	ReLU
	Dropout Rate	0.3
Training	Epoch	40
	Batch Size	128
	Train/Validation Split	0.2

training and inference is dominated by the training phase, which can be expressed as:

$$\text{Total Cost} = O(E \cdot (T \cdot (|S| \cdot |A| + F)))$$

DQN can become computationally expensive as the state and action spaces grow due to the need for extensive exploration and training to converge to an optimal policy. This makes DQN less scalable for large, complex networks.

### 7.0.3 SS-VAE

The complexity of training a VAE is  $O(E \cdot (D \cdot L + L^2))$ , where  $E$  is the number of epochs,  $D$  is the dimensionality of the input data, and  $L$  is the number of latent dimensions. The complexity of inferring resource allocations using a trained VAE is  $O(D \cdot L + L^2)$ . In addition, the complexity of training with contrastive loss is  $O(N \cdot D \cdot L)$ , where  $N$  is the number of samples. Combining both phases, the total computational cost of the SS-VAE method is:

$$\text{Total Cost} = O(E \cdot (D \cdot L + L^2)) + O(N \cdot D \cdot L)$$

The SS-VAE method scales efficiently with the number of features and samples due to its reliance on learning from data. While the training phase is computationally intensive, it is performed offline, and the inference phase is relatively lightweight, making it suitable for real-time applications in dynamic O-RAN environments.

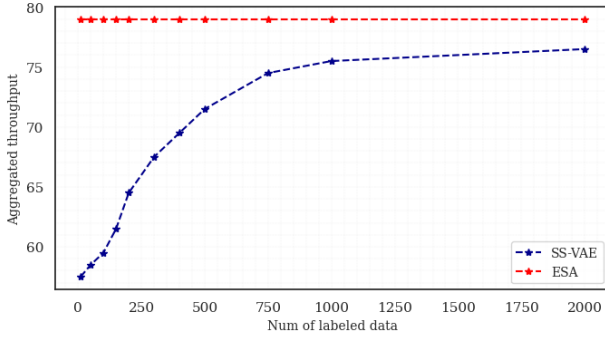
### 7.0.4 Comparison and Implications

The ESA guarantees finding the global optimal solution, but its computational infeasibility makes it impractical for large-scale networks. DQN provides a scalable solution; however, it requires extensive training and help with efficiency in large, complex networks. The SS-VAE method balances computational efficiency and scalability, making it suitable for real-time resource allocation in dynamic O-RAN environments. It achieves near-optimal performance with significantly lower computational costs, making it a robust and practical solution for modern O-RAN systems.

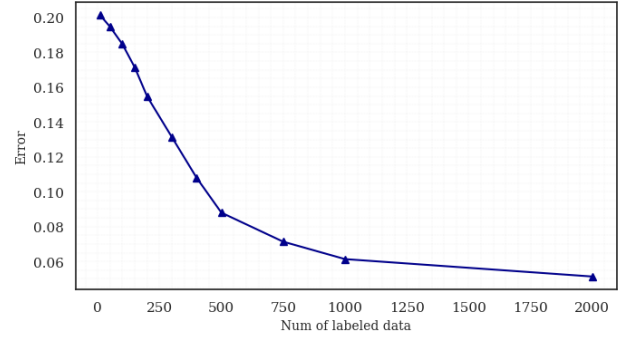
## 8 CONCLUSIONS

This paper introduced SS-VAE, a novel GAI framework for optimizing downlink O-RAN resource allocation and network slicing. SS-VAE coordinates xApps to manage RU associations, power, and PRBs, maximizing weighted throughput for eMBB and URLLC services. To tackle the NP-hard optimization challenge, SS-VAE employs a unified semi-supervised DNN. This architecture synergistically integrates

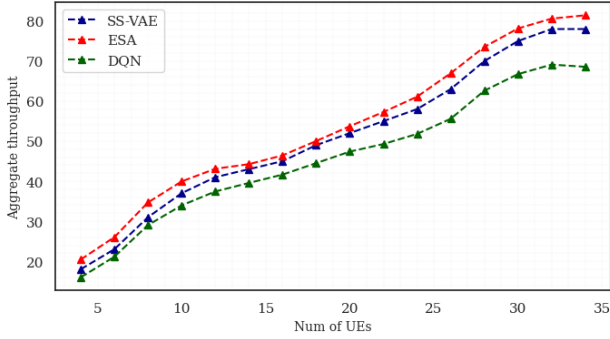




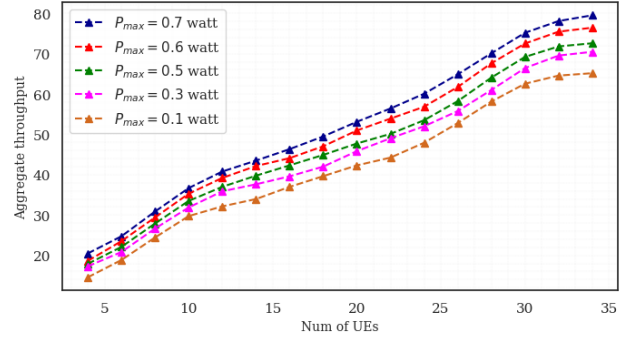
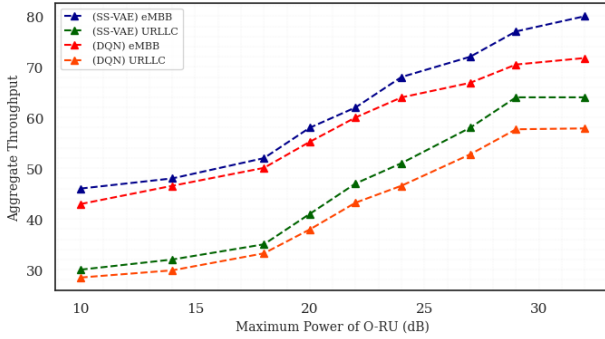
(a) Aggregated throughput of SS-VAE and ESA.



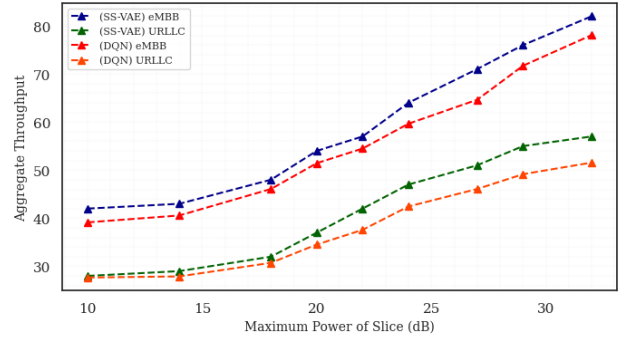
(b) Association error of SS-VAE and ESA.



(c) Aggregated throughput vs. number of UEs.

(d) Aggregated throughput vs. number of UEs ( $P_{O-RU}$ ).

(e) Aggregated throughput vs. O-RU power.



(f) Aggregated throughput vs. Power of slice.

Fig. 6: Simulation results showing various performance metrics and algorithm comparisons for SS-VAE, ESA, and DQN models.

a VAE—whose generative capabilities are honed using ESA-derived optimal parameters to determine allocation decisions—with a contrastive loss function that enhances representation learning, generalization, and robustness using both labeled and unlabeled data.

Evaluations against the ESA and DQN benchmarks demonstrated SS-VAE's ability to achieve near-optimal performance, comparable to ESA and significantly outperforming DQN while incurring the reduced computational cost. Our simulations confirmed the efficacy of SS-VAE in managing eMBB/URLLC QoS across diverse O-RAN scenarios. As a semi-supervised GAI framework, SS-VAE offers notable sample efficiency, robust generalization from limited data, and adaptability to dynamic conditions, marking it as a compelling solution for practical O-RAN deployments.

Future research will address end-to-end UE delay, investigate deployment costs, and incorporate UE mobility. We also aim to explore enhanced GAI techniques and other advanced AI or hybrid optimization algorithms to improve further resource allocation strategies in dynamic O-RAN systems, thereby opening new avenues for research in this evolving field.

## REFERENCES

- [1] L. M. Larsen, A. Checko, and H. L. Christiansen, "A survey of the functional splits proposed for 5G mobile crosshaul networks," *IEEE Communications Surveys & Tutorials*, vol. 21, no. 1, pp. 146–172, 2018.
- [2] O. Nassef, W. Sun, H. Purmehdi, M. Tatipamula, and T. Mahmoodi, "A survey: Distributed machine learning for 5g and beyond," *Computer Networks*, vol. 207, p. 108820, 2022.

- [3] S. Zhang, "An overview of network slicing for 5g," *IEEE Wireless Communications*, vol. 26, no. 3, pp. 111–117, 2019.
- [4] J. Zhao, Z. Zhu, Z. Huang, and B. Wang, "Multi-dimensional resource allocation algorithm for end-to-end network slicing," in *Industrial Engineering and Applications*. IOS Press, 2023, pp. 345–355.
- [5] X. Lin, "An overview of the 3gpp study on artificial intelligence for 5g new radio," *arXiv preprint arXiv:2308.05315*, 2023.
- [6] P. Popovski, K. F. Trillingsgaard, O. Simeone, and G. Durisi, "5g wireless network slicing for embb, urllc, and mmhc: A communication-theoretic view," *Ieee Access*, vol. 6, pp. 55765–55779, 2018.
- [7] J. Huang, F. Yang, C. Chakraborty, Z. Guo, H. Zhang, L. Zhen, and K. Yu, "Opportunistic capacity based resource allocation for 6g wireless systems with network slicing," *Future Generation Computer Systems*, vol. 140, pp. 390–401, 2023.
- [8] M. Al-Ali and E. Yaacoub, "Resource allocation scheme for embb and urllc coexistence in 6g networks," *Wireless Networks*, pp. 1–20, 2023.
- [9] A. S. Abdalla, P. S. Upadhyaya, V. K. Shah, and V. Marojevic, "Toward next generation open radio access networks: What o-ran can and cannot do!" *IEEE Network*, vol. 36, no. 6, pp. 206–213, 2022.
- [10] M. K. Shehzad, L. Rose, M. M. Butt, I. Z. Kovács, M. Assaad, and M. Guizani, "Artificial intelligence for 6g networks: Technology advancement and standardization," *IEEE Vehicular Technology Magazine*, vol. 17, no. 3, pp. 16–25, 2022.
- [11] M. K. Motalleb, C. Benzaid, T. Taleb, and V. Shah-Mansouri, "Moving target defense based secured network slicing system in the o-ran architecture," in *GLOBECOM 2023-2023 IEEE Global Communications Conference*. IEEE, 2023, pp. 6358–6363.
- [12] D. P. Kingma and M. Welling, "Auto-encoding variational bayes," *arXiv preprint arXiv:1312.6114*, 2013.
- [13] T. Chen, S. Kornblith, M. Norouzi, and G. Hinton, "A simple framework for contrastive learning of visual representations," in *International conference on machine learning*. PMLR, 2020, pp. 1597–1607.
- [14] "O-RAN: Towards an Open and Smart RAN, O-RAN Alliance White Paper, October 2018, O-RAN Alliance."
- [15] "Deploying 5G networks, 2020, Nokia corporation. Available at: <https://www.nokia.com/networks/5g/mobile/5g-resources/>."
- [16] A. Javadpour, F. Ja'fari, T. Taleb, and C. Benzaid, "Reinforcement learning-based slice isolation against ddos attacks in beyond 5g networks," *IEEE Transactions on Network and Service Management*, vol. 20, no. 3, pp. 3930–3946, 2023.
- [17] M. K. Motalleb, V. Shah-Mansouri, S. Parsaeefard, and O. L. A. López, "Resource allocation in an open ran system using network slicing," *IEEE Transactions on Network and Service Management*, vol. 20, no. 1, pp. 471–485, 2022.
- [18] L. Bonati, S. D'Oro, M. Polese, S. Basagni, and T. Melodia, "Intelligence and learning in o-ran for data-driven nextg cellular networks," *IEEE Communications Magazine*, vol. 59, no. 10, pp. 21–27, 2021.
- [19] M. K. Motalleb, C. Benzaid, T. Taleb, M. Katz, V. Shah-Mansouri, and J. Kim, "Towards secure intelligent o-ran architecture: vulnerabilities, threats and promising technical solutions using llms," *Digital Communications and Networks*, 2025.
- [20] L. Feng, Y. Zi, W. Li, F. Zhou, P. Yu, and M. Kadoch, "Dynamic resource allocation with ran slicing and scheduling for urllc and embb hybrid services," *Ieee Access*, vol. 8, pp. 34538–34551, 2020.
- [21] M. K. Motalleb, V. Shah-Mansouri, and S. N. Naghadeh, "Joint power allocation and network slicing in an open ran system," *arXiv preprint arXiv:1911.01904*, 2019.
- [22] N. Kazemifard and V. Shah-Mansouri, "Minimum delay function placement and resource allocation for open ran (o-ran) 5g networks," *Computer Networks*, vol. 188, p. 107809, 2021.
- [23] J. A. Hurtado Sánchez, K. Casilimas, and O. M. Caicedo Rendon, "Deep reinforcement learning for resource management on network slicing: A survey," *Sensors*, vol. 22, no. 8, p. 3031, 2022.
- [24] B. Adhikari, M. Jaseemuddin, and A. Anpalagan, "Resource allocation for co-existence of embb and urllc services in 6g wireless networks: A survey," *IEEE Access*, 2023.
- [25] Y.-H. Chen, "An adaptive heuristic algorithm to solve the network slicing resource management problem," *International Journal of Communication Systems*, vol. 36, no. 8, p. e5463, 2023.
- [26] F. Lotfi, H. Rajoli, and F. Afghah, "Llm-augmented deep reinforcement learning for dynamic o-ran network slicing," *environments*, vol. 2, p. 4, 2024.
- [27] A. Salama, M. M. Qazzaz, S. D. A. Shah, M. Hafeez, and S. A. Zaidi, "Fedora: Resource allocation for federated learning in oran using radio intelligent controllers," *arXiv preprint arXiv:2505.19211*, 2025.
- [28] C. Zhao, H. Du, D. Niyato, J. Kang, Z. Xiong, D. I. Kim, X. Shen, and K. B. Letaief, "Generative ai for secure physical layer communications: A survey," *IEEE Transactions on Cognitive Communications and Networking*, 2024.
- [29] Y. B. Uslu, S. Hadou, S. S. Bidokhti, and A. Ribeiro, "Generative diffusion models for resource allocation in wireless networks," *arXiv preprint arXiv:2504.20277*, 2025.
- [30] Z. Chen, Z. Zhang, and Z. Yang, "Big ai models for 6g wireless networks: Opportunities, challenges, and research directions," *IEEE Wireless Communications*, 2024.
- [31] J. Li, X. Zhang, J. Zhang, J. Wu, Q. Sun, and Y. Xie, "Deep reinforcement learning-based mobility-aware robust proactive resource allocation in heterogeneous networks," *IEEE Transactions on Cognitive Communications and Networking*, vol. 6, no. 1, pp. 408–421, 2019.
- [32] W. Wu, N. Chen, C. Zhou, M. Li, X. Shen, W. Zhuang, and X. Li, "Dynamic ran slicing for service-oriented vehicular networks via constrained learning," *IEEE Journal on Selected Areas in Communications*, vol. 39, no. 7, pp. 2076–2089, 2020.
- [33] X. Wang, J. D. Thomas, R. J. Piechocki, S. Kapoor, R. Santos-Rodríguez, and A. Parekh, "Self-play learning strategies for resource assignment in open-ran networks," *Computer Networks*, vol. 206, p. 108682, 2022.
- [34] A. Ndikumana, K. K. Nguyen, and M. Cheriet, "Federated learning assisted deep q-learning for joint task offloading and fronthaul segment routing in open ran," *IEEE Transactions on Network and Service Management*, 2023.
- [35] S. Mhatre, F. Adelantado, K. Ramantas, and C. Verikoukis, "Transfer learning applied to deep reinforcement learning for 6g resource management in intra-and inter-slice ran-edge domains," *IEEE Transactions on Consumer Electronics*, 2025.
- [36] Q. Chen and B. Heydari, "Resource governance in networked systems via integrated variational autoencoders and reinforcement learning," *arXiv preprint arXiv:2410.23393*, 2024.
- [37] K. Qiao, H. Wang, W. Zhang, D. Yang, Y. Zhang, and N. Zhang, "Resource allocation for network slicing in open ran: A hierarchical learning approach," *IEEE Transactions on Cognitive Communications and Networking*, 2025.
- [38] M. M. Qazzaz, Ł. Kułacz, A. Kliks, S. A. Zaidi, M. Dryjanski, and D. McLernon, "Machine learning-based xapp for dynamic resource allocation in o-ran networks," in *2024 IEEE International Conference on Machine Learning for Communication and Networking (ICMLCN)*. IEEE, 2024, pp. 492–497.
- [39] T. Erpek, A. Abdelhadi, and T. C. Clancy, "An optimal application-aware resource block scheduling in lte," in *2015 International Conference on Computing, Networking and Communications (ICNC)*. IEEE, 2015, pp. 275–279.
- [40] H. Eiselt, C.-L. Sandblom et al., *Nonlinear optimization*. Springer, 2019.
- [41] J. Nocedal and S. J. Wright, *Numerical optimization*. Springer, 1999.
- [42] A. Filali, B. Nour, S. Cherkaoui, and A. Kobbane, "Communication and computation o-ran resource slicing for urllc services using deep reinforcement learning," *IEEE Communications Standards Magazine*, vol. 7, no. 1, pp. 66–73, 2023.
- [43] A. Feriani and E. Hossain, "Single and multi-agent deep reinforcement learning for ai-enabled wireless networks: A tutorial," *IEEE Communications Surveys & Tutorials*, vol. 23, no. 2, pp. 1226–1252, 2021.
- [44] K. Suh, S. Kim, Y. Ahn, S. Kim, H. Ju, and B. Shim, "Deep reinforcement learning-based network slicing for beyond 5g," *IEEE Access*, vol. 10, pp. 7384–7395, 2022.
- [45] J. Fan, Z. Wang, Y. Xie, and Z. Yang, "A theoretical analysis of deep q-learning," in *Learning for dynamics and control*. PMLR, 2020, pp. 486–489.
- [46] D. P. Kingma, M. Welling et al., "An introduction to variational autoencoders," *Foundations and Trends® in Machine Learning*, vol. 12, no. 4, pp. 307–392, 2019.
- [47] D. P. Kingma and J. Ba, "Adam: A method for stochastic optimization," *arXiv preprint arXiv:1412.6980*, 2014.



- [48] C. Geng, N. Naderializadeh, A. S. Avestimehr, and S. A. Jafar, "On the optimality of treating interference as noise," *IEEE Transactions on Information Theory*, vol. 61, no. 4, pp. 1753–1767, 2015.
- [49] N. Naderializadeh and A. S. Avestimehr, "Itlinq: A new approach for spectrum sharing in device-to-device communication systems," *IEEE journal on selected areas in communications*, vol. 32, no. 6, pp. 1139–1151, 2014.
- [50] N. Naderializadeh, "Contrastive self-supervised learning for wireless power control," in *ICASSP 2021-2021 IEEE International Conference on Acoustics, Speech and Signal Processing (ICASSP)*. IEEE, 2021, pp. 4965–4969.
- [51] Q. Shi, M. Razaviyayn, Z.-Q. Luo, and C. He, "An iteratively weighted mmse approach to distributed sum-utility maximization for a mimo interfering broadcast channel," *IEEE Transactions on Signal Processing*, vol. 59, no. 9, pp. 4331–4340, 2011.
- [52] K. Janocha and W. M. Czarnecki, "On loss functions for deep neural networks in classification," *arXiv preprint arXiv:1702.05659*, 2017.
- [53] A. Paszke, S. Gross, F. Massa, A. Lerer, J. Bradbury, G. Chanan, T. Killeen, Z. Lin, N. Gimelshein, L. Antiga *et al.*, "Pytorch: An imperative style, high-performance deep learning library," *Advances in neural information processing systems*, vol. 32, 2019.
- [54] M. Elsayed and M. Erol-Kantarci, "Reinforcement learning-based joint power and resource allocation for urlc in 5g," in *2019 IEEE Global Communications Conference (GLOBECOM)*. IEEE, 2019, pp. 1–6.
- [55] R. Joda, T. Pamuklu, P. E. Iturria-Rivera, and M. Erol-Kantarci, "Deep reinforcement learning-based joint user association and cudo placement in o-ran," *IEEE Transactions on Network and Service Management*, vol. 19, no. 4, pp. 4097–4110, 2022.